

Chapter 8

Submarine Groundwater Discharge and its Influence on Primary Production in Japanese Coasts: Case Study in Obama Bay



Hisami Honda, Ryo Sugimoto, and Shiho Kobayashi

Abstract We report the relationship between submarine groundwater discharge (SGD) and primary production in the nearshore coast of Obama Bay, Japan, using three approaches. First, we conducted high-resolution mapping of ^{222}Rn and biogeochemical properties along the coast. The eastern part of the bay was strongly influenced by groundwater through several direct and indirect pathways. Lower $\delta^{15}\text{N}$ values in seaweed collected from the eastern area were indicative of larger influences of groundwater. Second, we measured the vertical distributions of ^{222}Rn , salinity, and chlorophyll-a (Chl-a) concentrations along two transects from onshore to offshore at two sites (Tomari and Kogasaki) located on the eastern coast of the bay. In Tomari, Chl-a concentrations were higher in the surface layer in the nearshore coastal area where ^{222}Rn and salinity showed higher and lower values, respectively, due to terrestrial spring water and SGD in the intertidal zone. In contrast, higher ^{222}Rn and Chl-a values were detected in the bottom layer in Kogasaki. This suggested that SGD was composed mainly of recirculated seawater discharge from the seafloor. Finally, temporal variations in multiple parameters related to SGD and phytoplankton production were recorded in Kogasaki in July and November. There was no clear relationship between tide and ^{222}Rn concentrations in either month, but $p\text{CO}_2$ and dissolved O_2 showed clear diurnal variations. The estimated O_2 production rate in July was higher than that in November. This seasonal difference may have been caused by differences in the SGD rate (7.1 cm d^{-1} in July and 3.7 cm d^{-1} in November).

H. Honda
Research Institute for Humanity and Nature, Kyoto, Japan
e-mail: h_honda@chikyu.ac.jp

R. Sugimoto (✉)
Department of Marine Bioscience, Faculty of Marine Bioscience, Fukui Prefectural University, Fukui, Japan
e-mail: sugiry@fpu.ac.jp

S. Kobayashi
Field Science Education and Research Center, Kyoto University, Kyoto, Japan
e-mail: shihok@kais.kyoto-u.ac.jp

Keywords Submarine groundwater discharge · ^{222}Rn · Nutrients · Primary production · Coastal seas

8.1 Introduction

8.1.1 Overview

Submarine groundwater discharge (SGD) is defined as terrestrially derived freshwater and recirculated seawater, which includes discharge associated with salt water intrusion along a coastline, tidal pumping, and wave setup, which flow out from the seabed into coastal water through underlying sediments (Destouni and Prieto 2003). Most estimates of terrestrially derived fresh SGD range from 6 to 10% of surface water inputs (Burnett et al. 2003). According to a recent report by Kwon et al. 2014, the total SGD, including fresh terrestrial groundwater and recirculated seawater, is 3 to 4 times greater than river water fluxes into the Atlantic and Indo-Pacific Oceans. Therefore, SGD is non-negligible, even from the perspective of the water cycle.

SGD is an important nutrient source for coastal ecosystems (Johannes 1980; Valiela et al. 1990). Nutrient concentrations in coastal groundwater are relatively higher than those in river water and seawater; therefore, even a small amount of groundwater discharge may contribute to nutrient budgets in coastal ecosystem (Burnett et al. 2003; Moore 2010). For example, nutrients transported through groundwater can support benthic and water column primary production in coastal seas such as sandy beaches and tidal flats (Kamermans et al. 2002; Miller and Ullman 2004; Paytan et al. 2006; Waska and Kim 2010; Waska and Kim 2011). In the coral reef off the west coast of Australia, SGD contributes significantly to reef productivity (Greenwood et al. 2013). In recent years, a direct relationship between SGD and *in situ* phytoplankton primary productivity in nearshore coastal areas in Japan has been clarified (Sugimoto et al. 2017). In addition, nutrient addition bioassay experiments support that SGD acts as a continual nutrient source (Gobbler and Boneillo 2003; Lecher et al. 2015). Conversely, it is well known that excess nutrient loadings via polluted groundwater into coastal seas cause cultural eutrophication and microalgal blooms (Pearl 1997; Gobler and Boneillo 2003).

8.1.2 Study Site

Obama Bay is a semi-enclosed embayment located in the central part of Wakasa Bay facing the Sea of Japan (Fig. 8.1). It has a surface area of 58.7 km², and is 17 km wide from east to west, 6 km wide from major river mouth to the bay mouth, and the bay mouth is 2.5 km wide. It has a volume of 0.74 km³ with a mean depth of 13 m. Shallow areas (<5 m depth) occupy 16% of the surface area (Sugimoto

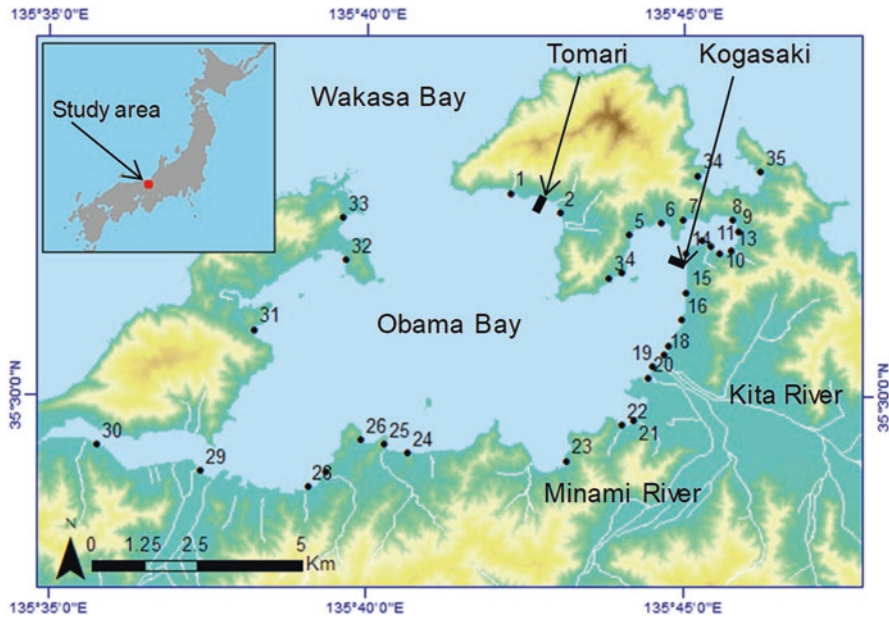


Fig. 8.1 Location of the study site, Obama Bay, Japan

We conducted the towing survey along the coast in March 2013. The dots and numbers indicate the *Ulva pertusa* sampling points in May 2012. We conducted the transect survey at two transects, as indicated bold lines, in Tomari and Kogasaki in July 2012. We conducted the mooring survey in Kogasaki in July and November 2013

et al. 2016). The volume of bay water exchange with the adjacent Wakasa Bay is about $2000 \text{ m}^3 \text{ s}^{-1}$ in summer, and the mean water residence time in summer is approximately 4 days (Sugimoto et al. 2016). Two major rivers, Kita River and Minami River, flow into the eastern part of the bay with a mean river discharge of approximately $10 \text{ m}^3 \text{ s}^{-1}$. The annual precipitation of the watershed is $>2000 \text{ mm year}^{-1}$ (Sugimoto and Tsuboi 2017). Meanwhile, the alluvial fan (i.e., Obama Plain) is formed along the Kita River, and there are substantial groundwater resources on this plain (Sasajima and Sakamoto 1962; Obama City 2017). More than 100 flowing artesian wells are found within the Obama Plain near the coast.

The fresh SGD rates flowing into Obama Bay were estimated based on monthly ^{222}Rn and salinity data using a steady state mass balance model. The annual mean rate was $0.36 \times 10^6 \text{ m}^3 \text{ day}^{-1}$ ($= 0.62 \text{ cm d}^{-1}$) with large intra-annual variability from 0.05×10^6 to $0.77 \times 10^6 \text{ m}^3 \text{ day}^{-1}$, which was relatively high in spring (March–April), when snowmelt water was predominant, and in the rainy summer season (June–September) (Sugimoto et al. 2016). The mean fresh SGD rate corresponded with the result based on seepage meter measurements in the nearshore coast (0.41 cm d^{-1}) and the total SGD rate was approximately 4.6 cm d^{-1} (Kobayashi et al. 2017). Comparing the nutrient concentrations in terrestrial groundwater with those in river water, dissolved inorganic nitrogen (DIN) and phosphorus (DIP)

concentrations in groundwater were about 2 times and 7 times higher than those of river water, respectively. The resulting mean fluxes of DIN, DIP, and dissolved silica (DSi) via SGD were 42.8 kg day^{-1} (range: $64.7\text{--}947.1 \text{ kg day}^{-1}$), 38.0 kg day^{-1} ($5.6\text{--}81.4 \text{ kg day}^{-1}$), and $914.2 \text{ kg day}^{-1}$ ($133.6\text{--}1955.6 \text{ kg day}^{-1}$), respectively. The mean fractions of groundwater in the total terrestrial fluxes of DIN, DIP, and DSi were 42.4% (9.0–72.2%), 65.3% (26.1–87.6%), and 33.4% (6.6–61.6%), respectively (Sugimoto et al. 2016).

DIP-enriched groundwater discharge could represent a non-negligible nutrient source for primary production in Obama Bay, since primary production is mostly restricted by phosphorous throughout the year (Sugimoto et al. 2016). Sugimoto et al. (2017) revealed the direct relationship between SGD and *in situ* primary production of phytoplankton. They conducted *in situ* measurements of primary productivity using a stable ^{13}C tracer method and environmental parameters (e.g., ^{222}Rn concentration, light intensity, temperature, and nutrient concentrations) at six stations in summer. They found a significant relationship between primary productivity and ^{222}Rn concentration. Although light intensity and water temperature differed at each station and in each month, nutrient concentrations limited primary productivity. Honda et al. (2016) also determined the sudden groundwater discharge and associated chlorophyll peak in the bottom layer (depth: 18 m) around 2 km offshore from the river mouth in June 2011, one week after a notable flood (Fig. 8.2). These results indicate that the nutrient supply from SGD has a crucial impact on primary production in Obama Bay.

8.1.3 Objectives

In this chapter, we show the relationship between SGD and primary production in the nearshore coastal area of Obama Bay using three approaches based on the above-mentioned method. First, we conducted a spatial assessment of SGD and biogeochemical parameters in the nearshore coastal area using a towing survey. A method of continuously monitoring active ^{222}Rn concentrations in water has been developed and used to visualize the distribution of groundwater discharge into coastal seas (Burnett et al. 2001; Burnett and Dulaiova 2003). Based on this method, in this study, we conducted high-resolution mapping of ^{222}Rn and biogeochemical properties along the coast of Obama Bay. Moreover, we used the $\delta^{15}\text{N}$ values of seaweed as an indicator of nutrient inputs through SGD, as they assimilate and accumulate nutrients from the water column, integrating continuous and pulsed nutrient loadings.

Second, transect surveys from nearshore to offshore at two sites (Tomari and Kogasaki in Fig. 8.1) were conducted. The eastern coast of the bay has a few streams, but freshwater springs on land and groundwater discharge at the intertidal zone exist along the coast of these areas.

Finally, we evaluated the diurnal variation in SGD and primary production in summer and autumn at Kogasaki (Fig. 8.1). Recent technological advances (i.e.,

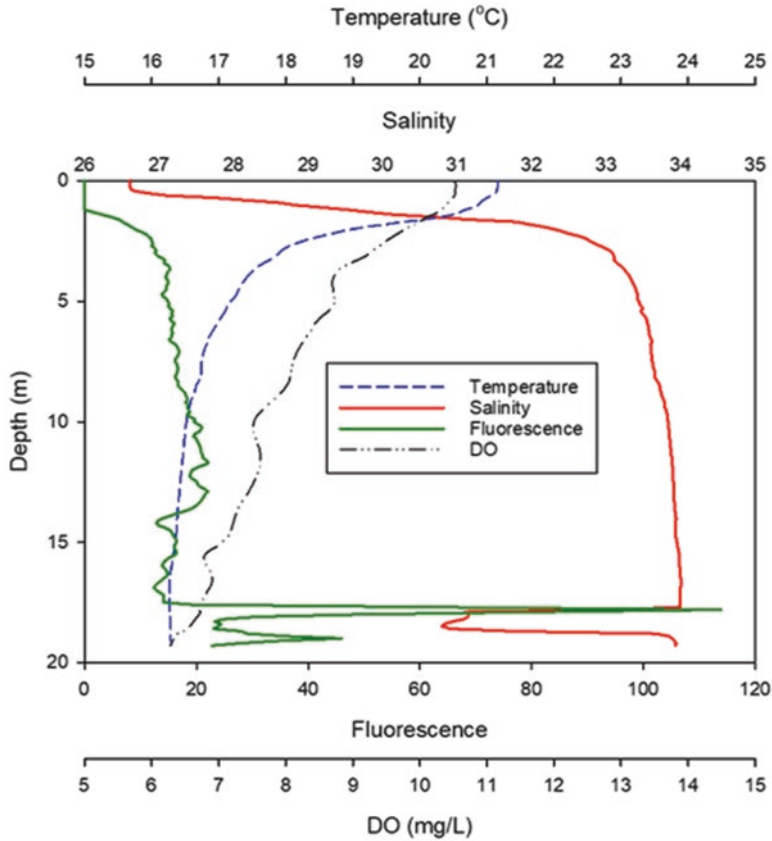


Fig. 8.2 Vertical profiles of temperature, salinity, chlorophyll fluorescence, and dissolved O₂ (DO) in the central part of Obama Bay on 7 June 2011. (Modified from Honda et al. 2016)

automation) have increased the ability to assess SGD in coastal ecosystems using natural tracers such as ²²²Rn. Simultaneous monitoring of ²²²Rn with indicators of primary production such as *p*CO₂, dissolved O₂ and chlorophyll-a (Chl-a) enabled us to determine the relationship between these processes.

8.2 Materials and Methods

8.2.1 Towing Survey

To detect SGD and to estimate the biogeochemical influence of SGD on primary producers in the nearshore coastal area of Obama Bay, the spatial distributions of ²²²Rn, salinity, and nutrient concentrations were investigated along the coast on 13,

15, and 16 March 2013. We applied the multidetector method (Dulaiova et al. 2005; Stieglitz et al. 2010) for continuous ^{222}Rn measurements using three radon detectors (RAD7, DurrIDGE) at a boat velocity of about 1–2 knots with water depths of around 2 m. We used two sets of three radon detectors, with a measurement interval of 10 min for each system; therefore, the average values and standard deviations of the ^{222}Rn concentrations were obtained every 5 min. Temperature and salinity were simultaneously measured every 1 min using the conductivity and temperature logger (AAQ1183, JFE-Advantech). Seawater samples for nutrient concentrations were collected every 10 min. In the laboratory, concentrations of NO_3^- , NO_2^- , PO_4^{3-} , and DSi were measured using an auto-analyzer (QuAAtro, BL-Tech). The concentration of NH_4^+ was measured using a fluorometer (Trilogy, Turner Design). In this study, we defined DIN as the sum of NO_3^- , NO_2^- and NH_4^+ , and DIP as PO_4^{3-} .

Seaweed (*Ulva pertusa* Areschoug) was collected from 33 coastal sites in the bay and two sites outside the bay (numbers 1 to 35 in Fig. 8.1). The $\delta^{15}\text{N}$ values of *U. pertusa* were analyzed using a PDZ Europa ANCA-GSL elemental analyzer interfaced to a PDZ Europa 20–20 isotope ratio mass spectrometer (Sercon) at the University of California-Davis Stable Isotope Facility.

8.2.2 Transect Survey

The vertical distributions of temperature, salinity, and chlorophyll fluorescence were measured in two transects from onshore to offshore in Tomari on 24 July 2012 and Kogasaki on 29 July 2012 (locations shown in Fig. 8.1), using a CTD instrument (AAQ1183, JFE Advantech). Along each transect, six stations were set up at the points where the water depths were 0, 1, 2, 3, 4, and 5 m. Seawater was sampled at the surface and 0.5 m above the sea bottom of each station using a 6-L Van Dorn water sampler (RIGO Co., Ltd.). Seawater samples were filtered through 0.7- μm glass fiber filter (GF/F, Whatman) and the concentration of Chl-a on the GF/F filters was quantified with a calibrated fluorometer (Trilogy, Turner Design) to calibrate the chlorophyll fluorescence sensor attached to the CTD instrument. The ^{222}Rn concentrations of bottle samples were measured using the RAD7 detector.

8.2.3 Mooring Survey

The temporal variations of the parameters related to SGD and phytoplankton production were recorded in Kogasaki from 9 to 11 July 2013 and from 15 to 16 November 2013. To measure ^{222}Rn and $p\text{CO}_2$ simultaneously, seawater was pumped via a submersible pump into a gas equilibration chamber (RAD Aqua, DurrIDGE), where the headspace of the equilibrated gas was measured using mobile ^{222}Rn (RAD7, DurrIDGE) and CO_2 (GMP343, Vaisala) detectors. ^{222}Rn and $p\text{CO}_2$ were

measured every 10 min and 5 min, respectively. Temperature, salinity, and dissolved O_2 were measured using a multi-parameter sonde (ProPlus, YSI), and depth and light intensity were measured using data loggers (DEFI-DHG and DEFI-L, JFE Advantech) with a measurement interval of 5 min. The Chl-a concentration was measured every 5 min using a calibrated fluorescence sensor (Cyclops-7, Turner). For the atmospheric conditions, ^{222}Rn and CO_2 concentrations were measured using the aforementioned detectors. In this study, all data were averaged to 1-h data to remove short-term variability.

8.3 Results and Discussion

8.3.1 Towing Survey

The integrated map of the 3-day survey performed in March 2013 showed that the ^{222}Rn ranged from 0 to 347 Bq m^{-3} (Fig. 8.3a). Higher concentrations were measured in the eastern area, relatively high ($>150 \text{ Bq m}^{-3}$) concentrations were present in the zones between No.2 to No.14 and No.18 to No.22 (Figs. 8.1, 8.3a). The mean value and standard deviation of ^{222}Rn concentrations in the eastern area of the bay was $162 \pm 56 \text{ Bq m}^{-3}$, much higher than that in the western area ($203 \pm 37 \text{ Bq m}^{-3}$). The spatial variability in salinity ranged from 22.6 to 32.5, and lower salinity was found in the eastern area (Fig. 8.3b). Salinity showed a significant negative correlation with ^{222}Rn ($r = -0.47$, $p < 0.05$). The DIN, DIP, and DSi concentrations were higher in the eastern area, similar to the ^{222}Rn concentrations (Figs. 8.3c, d, e). DIN and DSi concentrations were particularly high in the zone between No.5 and No.10 (Figs. 8.1, 8.3c, e), while DIP concentrations were higher in the zone between No. 15 and No.23 (Figs. 8.1, 8.3c). ^{222}Rn was significantly positively correlated with DIN ($r = 0.47$, $p < 0.01$) and DSi ($r = 0.34$, $p < 0.05$), whereas no significant correlation between ^{222}Rn and DIP was observed ($r = 0.08$, $p = 0.57$).

The ^{222}Rn and nutrient concentrations in the eastern area were markedly higher than those in the western area. As noted by Kobayashi et al. (2017), there are two major sources of ^{222}Rn in Obama Bay, river water, which has high ^{222}Rn concentrations, and groundwater discharge offshore areas at the mouths of the Kita and Minami Rivers. The ^{222}Rn concentration in river water was one order of magnitude higher than that in seawater, because groundwater seeped from the riverbed. The ^{222}Rn concentrations along the coast ranged from 0 to 346.7 Bq m^{-3} , while the mean ^{222}Rn concentrations obtained from monthly river sampling were 1800 and 1200 Bq m^{-3} , respectively (Sugimoto et al. 2016). In Obama Bay, river water is dispersed sufficiently into the bay before ^{222}Rn supplied from the rivers has decayed (Kobayashi et al. 2017). In addition, the northward wind enhances the advection of the water high in ^{222}Rn supplied from the river toward the eastern area of the bay (Kobayashi et al. 2017). This effect is significant because March has the highest mean river discharge. Terrestrial groundwater discharge and/or recirculated seawater discharge

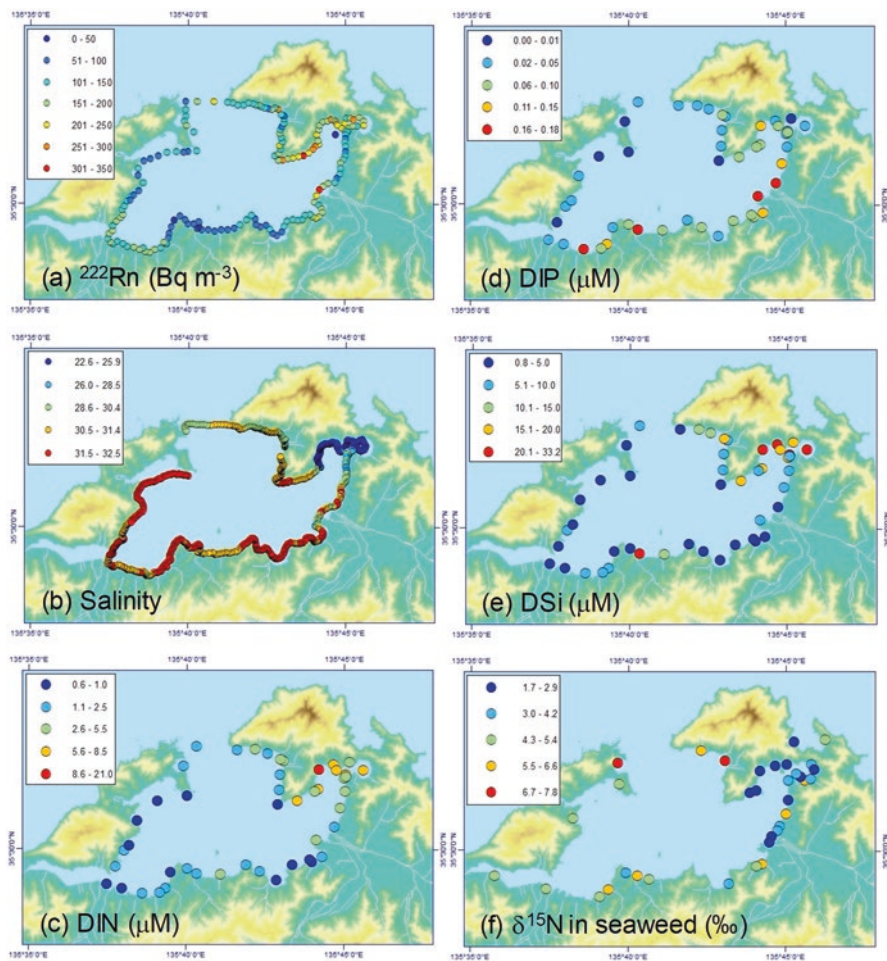


Fig. 8.3 Distributions of (a) ^{222}Rn , (b) salinity, (c) DIN, (d) DIP, and (e) DSi concentrations in surface water during 13, 15, and 16 March 2013 and (f) $\delta^{15}\text{N}$ in seaweed (*Ulva pertusa*) collected on 7, 8, and 11 May 2012

offshore the estuary represents another presumable source of water high in ^{222}Rn . PO_4^{3-} and ^{222}Rn concentrations were both higher in the zone between No.19 and No.22. This was considered to indicate the presence of significant SGD inputs, because PO_4^{3-} concentrations are higher in terrestrial groundwater than in river water (Sugimoto et al. 2016).

$\delta^{15}\text{N}$ values of primary producers such as phytoplankton, seaweed, and seagrass reflect the $\delta^{15}\text{N}$ of substrate nitrogen (Costanzo et al. 2001). The $\delta^{15}\text{N}$ values of *U. pertusa* ranged from 1.7 to 7.9‰ (Fig. 8.3e). The $\delta^{15}\text{N}$ values of *U. pertusa* around the eastern part of the bay ($2.9 \pm 1.1\text{‰}$) were significantly lower than those in other sites ($5.2 \pm 1.3\text{‰}$) ($p < 0.001$, t -test). Although we could not differentiate the $\delta^{15}\text{N}$

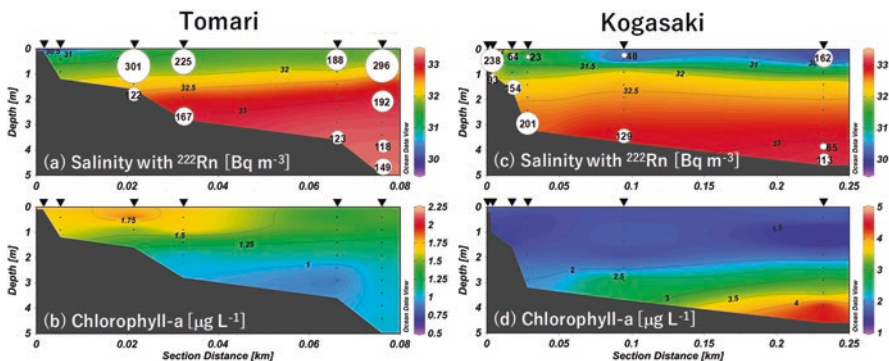


Fig. 8.4 Distributions of salinity (contour) with ^{222}Rn (circle: *top panels*) and Chl-a (*bottom panels*) in the transect of Tomari and Kogasaki on 24 and 29 July 2012. Triangles indicate the locations of the observation points

values of NO_3^- ($\delta^{15}\text{N}_{\text{NO}_3}$) obtained from terrestrial freshwater ($\delta^{15}\text{N}_{\text{NO}_3} = 3.7\text{‰}$ of river, $\delta^{15}\text{N}_{\text{NO}_3} = 3.6\text{‰}$ of spring water; Kobayashi, unpublished), the $\delta^{15}\text{N}_{\text{NO}_3}$ values of terrestrial freshwater were lower than those in oceanic waters of the Sea of Japan ($5.4 \pm 0.2\text{‰}$; Nakanishi and Minagawa 2003). These results imply that *U. pertusa* in the eastern part of the bay assimilate nitrogenous nutrients supplied from land, including groundwater.

8.3.2 Transect Survey

The ^{222}Rn concentrations in each zone separated by distance from the land and the vertical distributions of ^{222}Rn , salinity, and Chl-a along the two transects at Tomari and Kogasaki are shown in Fig. 8.1. Along the Tomari transect (Figs. 8.4a, b), the highest ^{222}Rn concentration (301 Bq m^{-3}) was observed around the stations closest to land. ^{222}Rn concentrations were higher at the surface than at the bottom along the transect. The vertical differences in the surface and bottom temperature were around $5 \text{ }^\circ\text{C}$, suggesting that the influence of tidal mixing was not significant, although the section was in the shallow zone ($>5 \text{ m}$). Salinity was low in the surface layer but high at the bottom, suggestive of river water flowing into the sea from the land, although there was no river or stream near this section. The Chl-a concentrations were relatively high in the surface layer, corresponding to the distribution of low-salinity water and ^{222}Rn .

Along the Kogasaki transect (Figs. 8.4c, d), ^{222}Rn concentrations were higher in the bottom layer than in the surface layer, except for the station closest to land. Salinity was lowest at the station farthest from land in the surface layer, suggestive of the influence of the advection of low-salinity water from the main rivers (Kobayashi et al. 2017). The highest Chl-a concentrations were observed in the bot-

tom layer at the station farthest from land, and Chl-a concentrations were higher in the bottom layer than in the surface layer, corresponding to the distribution of ^{222}Rn .

The relatively high ^{222}Rn concentrations and low salinity at the surface in Tomari indicated the influence of inflow from groundwater springs on land or SGD in the intertidal zone. In contrast, the relatively high concentrations of ^{222}Rn at the bottom unaccompanied by low salinity in Kogasaki suggested the influence of SGD mainly consisting of recirculated SGD, which has been observed in this area using a seepage meter (Kobayashi et al. 2017). In addition to river water, SGD is known to supply nutrients that are needed for phytoplankton growth in Obama Bay (Sugimoto et al. 2016; Honda et al. 2016).

Sugimoto et al. (2017) and Kobayashi et al. (2017) identified significant correlations between ^{222}Rn concentration and the primary production rate and ^{222}Rn and Chl-a, respectively, in the entire Obama Bay. The correlation between ^{222}Rn and Chl-a concentrations along the transects from the land toward offshore obtained in this study also suggest that groundwater influences primary production in the shallow zone along the coast. Although the link between ^{222}Rn and the primary production rate and the influence of the seawater residence time on the distributions of both ^{222}Rn and Chl-a must be clarified in future studies, the results of this survey provide persuasive evidence of the influence of SGD on primary production in the shallow zone of Obama Bay.

8.3.3 Mooring Survey

There were no significant differences in the mean water depth and tidal ranges in July and November, although the water temperature and salinity in July were considerably higher than those in November (Fig. 8.5). The ^{222}Rn concentration of $62 \pm 9 \text{ Bq m}^{-3}$ (mean \pm standard deviation) (range: 42–87 Bq m^{-3}) in July was significantly lower than that in November ($71 \pm 11 \text{ Bq m}^{-3}$, range: 54–92 Bq m^{-3}) ($p < 0.001$, t -test). There was no clear relationship between tide and ^{222}Rn concentration in either month.

Variations in the time-series ^{222}Rn record from the mooring survey were used to estimate the SGD flux with a non-steady-state mass balance model, as follows (Burnett and Dulaiova 2003; Hosono et al. 2012):

$$F_{\text{benthic}} - \lambda I_{\text{exRn}} - F_{\text{atm}} \pm F_{\text{hor}} = 0 \quad (8.1)$$

where F_{benthic} is the combined advective and diffusive flux of ^{222}Rn to the overlying water column, λ is the decay constant of ^{222}Rn ($= 0.181 \text{ d}^{-1}$), I_{exRn} is the inventory of excess ^{222}Rn concentration ($= ^{222}\text{Rn} - ^{226}\text{Ra}$), F_{atm} is the flux of ^{222}Rn to the atmosphere, and F_{hor} is the horizontal mixing of ^{222}Rn into or out of the mooring site.

The excess ^{222}Rn activities (unsupported by ^{226}Ra) in the water column were estimated by subtracting the single measured ^{226}Ra concentration of offshore water (7.7 Bq m^{-3} ; Sugimoto et al. 2016). Decay was not considered because the fluxes

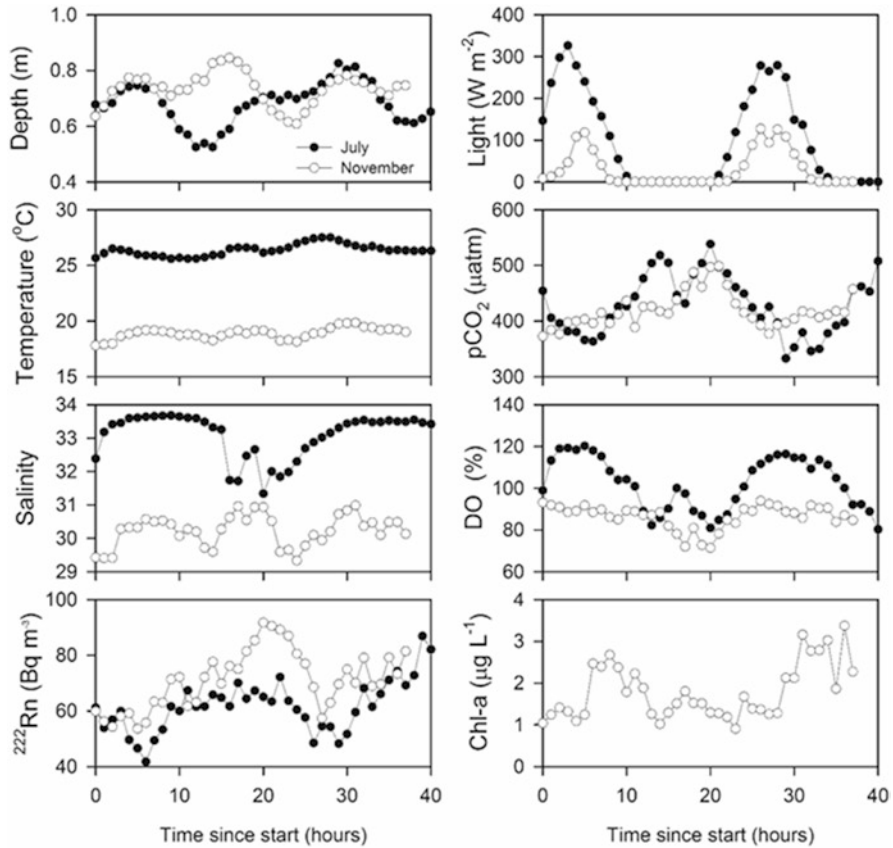
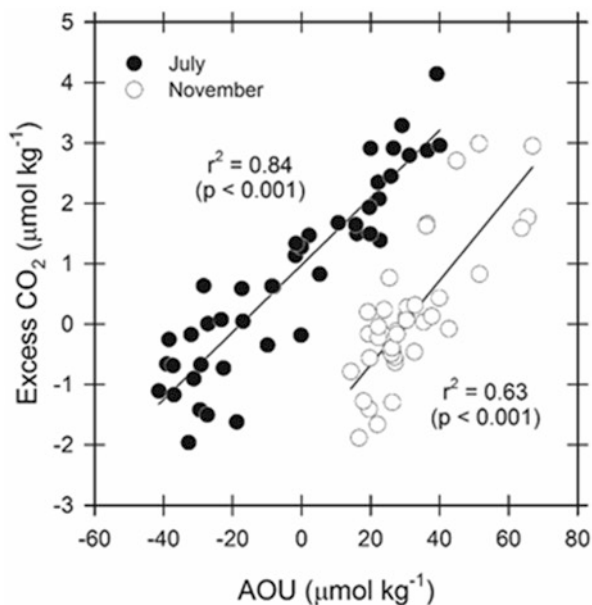


Fig. 8.5 Time series of water depth, temperature, salinity, ^{222}Rn concentration, light intensity, $p\text{CO}_2$, dissolved O_2 , and Chl-a concentration in July and November 2013. All data are shown beginning at 09:00 LST

were evaluated on a very short (1-h) time scale relative to the half-life of ^{222}Rn . F_{atm} was determined based on molecular diffusion and turbulent transfer models (MacIntyre et al. 1995; Wanninkhof 1992; Turner et al. 1996), and detailed calculations referred to those in Sugimoto et al. (2016). Atmospheric ^{222}Rn was assumed to be zero, and air temperature and wind speed data were derived from Japan Meteorological Agency reports. During the mooring survey period, these values ranged from 23.0 to 33.9°C and 0.6 to 4.0 m s^{-1} in July and from 8.6 to 16.9°C and 0.1 to 3.3 m s^{-1} in November, respectively. To calculate water flux, we simply divided F_{benthic} by ^{222}Rn activity in shallow groundwater around 10 m inland from the coast (3470 Bq m^{-3}). We assumed that advective flux of radon from the sediment dominated the total flux, and diffusive flux was ignored in our calculations.

The estimated SGD rates were $8.3 \pm 3.2 \text{ cm d}^{-1}$ in July and $6.3 \pm 3.3 \text{ cm d}^{-1}$ in November. In contrast to ^{222}Rn concentrations, the SGD rates in July were higher than those in November ($p = 0.017$, t -test), because apparent ^{222}Rn loss to atmo-

Fig. 8.6 Plots of apparent oxygen utilization (AOU) versus excess CO₂ in July and November 2013



sphere was higher in July. The SGD fluxes estimated from ²²²Rn were similar to those estimated with a seepage meter at the same site (4.6 cm d⁻¹; Kobayashi et al. 2017). The difference in SGD rates in July and November could affect primary production in the overlying water column.

*p*CO₂ and dissolved O₂ showed clear diurnal variations, and were lower and higher in daytime than at night, respectively (Fig. 8.5). These inverse trends are suggestive of the influence of phytoplankton photosynthesis and respiration. To facilitate the discussion, we defined the free dissolved CO₂ from atmospheric equilibrium as excess CO₂ (Eq. (8.2)) and the oxygen as apparent oxygen utilization (AOU) as Eq. ((8.3), following the method of Zhai et al. (2005).

$$\text{ExcessCO}_2 = [\text{CO}_2^*] - K_{\text{H}}^{\text{CO}_2} \times p\text{CO}_2 (\text{in air}) \quad (8.2)$$

where [CO₂*] is the concentration of total free CO₂ (i.e., [CO₂*] = [CO₂] + [H₂CO₃] = K_H^{CO₂} × *p*CO₂ in water) and K_H^{CO₂} is the solubility coefficient of CO₂.

$$\text{AOU} = [\text{O}_2]_{\text{eq}} - [\text{O}_2] \quad (8.3)$$

where [O₂]_{eq} is the DO concentration at equilibrium with the atmosphere and [O₂] is the *in situ* DO concentration.

AOU and excess CO₂ showed positive correlations in both months (Fig. 8.6). These clear trends support that the processes of photosynthesis and respiration control the temporal variations in *p*CO₂ and dissolved O₂. However, the variability of CO₂ and O₂ due to photosynthesis and respiration in seawater is generally assessed

Table 8.1 Average data of O₂ production rate, SGD, and limitation factors of temperature (F_T) and light (F_I) from 05:00 to 11:00 LST in July and November 2013

	O ₂ production ($\mu\text{mol kg}^{-1} \text{h}^{-1}$)	SGD (cm d^{-1})	F_T	F_I
July	11.2	7.1 ± 2.9	1.00 ± 0.00	0.61 ± 0.31
November	7.9	3.7 ± 1.4	0.96 ± 0.00	0.44 ± 0.41

Optimum temperature and light are assumed to be 25°C and 104.7 W m⁻²

by examining the relationship between total CO₂ (sum of CO₂^{*}, HCO₃⁻, and CO₃²⁻) and O₂ (DeGrandpre et al. 1997). To evaluate the stoichiometric relationship between total CO₂ and O₂, additional direct measurements such as alkalinity are needed for future studies.

In this study, we evaluated photosynthesis as the O₂ production rate using the AOU data. From 05:00 to 11:00 LST (integrated time from 21 to 27 of each month), when light intensity increased from near zero to the maximum, dissolved O₂ showed a linear increasing trend in both months (Fig. 8.5). The slopes in this period were $-11.2 \mu\text{mol AOU kg}^{-1} \text{h}^{-1}$ in July ($r^2 = 0.98$) and $-7.9 \mu\text{mol AOU kg}^{-1} \text{h}^{-1}$ in November ($r^2 = 0.91$). The SGD rate during the same period in July was 7.1 cm d⁻¹, which was considerably higher than that in November (Table 8.1). As noted by Kobayashi et al. (2017), nutrients are major limitation factor at the mooring site. Therefore, nutrients supplied from SGD could induce the difference in O₂ production rates (photosynthesis) in July and November. Since seasonal differences in light availability and water temperature may affect the difference in the O₂ production rate in July and November, we evaluated the limitation factors of light (F_I) and temperature (F_T) following the method of Sugimoto et al. (2017). As a result, light availability (0.61 in July and 0.44 in November, Table 8.1) may be a non-negligible environmental factor of lower O₂ production rate in November. However, simultaneous measurements of multiple parameters related SGD and primary production in future studies will lead to a better understanding of the roles of SGD on coastal ecosystems.

8.4 Conclusion

In this chapter, we presented the relationship between SGD and primary production in the nearshore coastal area of Obama Bay, Japan, using three approaches: towing, transect, and mooring surveys. Although the results collected in each approach support earlier findings and are thought to be correct, the results should be considered somewhat preliminary due to their collection within a few days and deficiency for individual use. Our recent papers (i.e., Honda et al. 2016; Kobayashi et al. 2017; Sugimoto et al. 2017) provide more comprehensive results. Considering that nearshore coastal areas have high productivity and biodiversity and many environmental issues, such as harmful algal blooms and alteration of the coast, occurs at this active area, the results in this chapter are highly suggestive and show the need for specific

surveys in nearshore coastal sites. In the near future, SGD studies will be expected to become considered an essential component of understanding coastal ecosystems.

Acknowledgment The transect survey from onshore to offshore in two transects were made in collaboration with Wakasa High School. We are grateful to the diving club members and their teachers, Dr. Yasuyuki Kosaka and Mr. Hiroaki Hirayama, and the headmaster of Wakasa High School for their assistance. This research was financially supported by the R-08-Init Project, entitled "Human-Environmental Security in Asia-Pacific Ring of Fire: Water-Energy-Food Nexus" the Research Institute for Humanity and Nature (RIHN), Kyoto, Japan.

References

- Burnett WC, Dulaiova H (2003) Estimating the dynamics of groundwater input into the coastal zone via continuous radon-222 measurements. *J Environ Radioact* 69:21–35
- Burnett WC, Kim G, Lane-Smith D (2001) A continuous monitor for assessment of ^{222}Rn in the coastal ocean. *J Radioanal Nucl Chem* 249:167–172
- Burnett WC, Bokuniewicz H, Huettel M, Moore WS, Taniguchi M (2003) Groundwater and pore water inputs to the coastal zone. *Biogeochemistry* 66:3–33
- Costanzo SD, O'Donohue MJ, Dennison WC, Loneragan NR, Thomas M (2001) A new approach for detecting and mapping sewage impacts. *Mar Pollut Bull* 42:149–156
- DeGrandpre MD, Hammar TR, Wallace DWR, Wirick CD (1997) Simultaneous mooring-based measurements of seawater CO_2 and O_2 off Cape Hatteras, North Carolina. *Limnol Oceanogr* 42:21–28
- Destouni G, Prieto C (2003) On the possibility for generic modeling of submarine groundwater discharge. *Biogeochemistry* 66:171–186
- Dulaiova H, Peterson R, Burnett WC, Lane-Smith D (2005) A multi-detector continuous monitor for assessment of ^{222}Rn in the coastal ocean. *J Radioanal Nucl Chem* 263:361–365
- Gobler CJ, Boneillo GE (2003) Impacts of anthropogenically influenced groundwater seepage on water chemistry and phytoplankton dynamics within a coastal marine system. *Mar Ecol Prog Ser* 255:101–114
- Greenwood JE, Symonds G, Zhong L, Lourey M (2013) Evidence of submarine groundwater nutrient supply to an oligotrophic barrier reef. *Limnol Oceanogr* 58:1834–1842
- Honda H, Sugimoto R, Kobayashi S, Tahara D, Tominaga O (2016) Temporal and spatial variation in primary production in Obama Bay. *Bull Jpn Soc Fish Oceanogr* 80:269–282. (in Japanese with English abstract)
- Hosono T, Ono M, Burnett WC, Tokunaga T, Taniguchi M, Akimichi T (2012) Spatial distribution of submarine groundwater discharge and associated nutrients within a local coastal area. *Environ Sci Technol* 46:5319–5326
- Johannes RE (1980) The ecological significance of the submarine discharge of groundwater. *Mar Ecol Prog Ser* 3:365–373
- Kamermans P, Hemminga MA, Tack JF, Mateo MA, Marbà N, Mtolera M, Stapel J, Verheyden A, Van Daele T (2002) Groundwater effects on diversity and abundance of lagoonal seagrasses in Kenya and on Zanzibar Island (East Africa). *Mar Ecol Prog Ser* 231:75–83
- Kobayashi S, Sugimoto R, Honda H, Miyata Y, Tahara D, Tominaga O, Shoji J, Yamada M, Nakada S, Taniguchi M (2017) High-resolution mapping and time-series measurements of ^{222}Rn concentrations and biogeochemical properties related to submarine groundwater discharge along the coast of Obama Bay, a semi-enclosed sea in Japan. *Prog Earth Planet Sci*. <https://doi.org/10.1186/s40645-017-0124-y>
- Kwon EY, Kim G, Primeau F, Moore WS, Cho HM, DeVries T, Sarmiento JL, Charette MA, Cho YK (2014) Global estimate of submarine groundwater discharge based on an observationally constrained radium isotope model. *Geophys Res Lett* 41:8438–8444

- Lecher AL, Mackey K, Kudela R, Ryan J, Fisher A, Murray J, Paytan A (2015) Nutrient loading through submarine groundwater discharge and phytoplankton growth in Monterey Bay, CA. *Environ Sci Technol* 49:6665–6673
- MacIntyre S, Wanninkhof R, Chanton JP (1995) Trace gas exchange across the air-sea interface in freshwater and coastal marine environments. In: Matson PA, Harris RC (eds) *Biogenic trace gases: measuring emissions from soil and water*. Blackwell Science, pp 52–97
- Miller DC, Ullman WJ (2004) Ecological consequences of ground water discharge to Delaware Bay, United States. *Groundwater* 42:959–970
- Moore WS (2010) The effect of submarine groundwater discharge on the ocean. *Annu Rev Mar Sci* 2:59–88
- Nakanishi T, Minagawa M (2003) Stable carbon and nitrogen isotopic compositions of sinking particles in the northeast Japan Sea. *Geochem J* 37:261–275
- Obama City (2017) <http://www1.city.obama.fukui.jp/category/page.asp?Page=3741>
- Paytan A, Shellenbarger GG, Street JH, Gonnera ME, Davis K, Young MB, Moore WS (2006) Submarine groundwater discharge: an important source of new inorganic nitrogen to coral reef ecosystems. *Limnol Oceanogr* 51:343–348
- Pearl HW (1997) Coastal eutrophication and harmful algal blooms: importance of atmospheric deposition and groundwater as “new” nitrogen and other nutrient sources. *Limnol Oceanogr* 42:1154–1165
- Sasajima S, Sakamoto K (1962) Subsurface geology and groundwater of Obama plain, Fukui pref., central Japan. Part 2: groundwater of Obama plain. *Memoirs of the Faculty of Liberal Arts, University of Fukui. Ser. II Natural science* (in Japanese with English abstract)
- Stieglitz TC, Cook PG, Burnett WC (2010) Inferring coastal processes from regional-scale mapping of 222 Radon and salinity: examples from the great barrier reef, Australia. *J Environ Radioact* 101:544–552
- Sugimoto R, Tsuboi T (2017) Seasonal and annual fluxes of atmospheric nitrogen deposition and riverine nitrogen export in two adjacent contrasting rivers in central Japan facing the sea of Japan. *J Hydro Reg Stud* 11:117–125
- Sugimoto R, Honda H, Kobayashi S, Takao Y, Tahara D, Tominaga O, Taniguchi M (2016) Seasonal changes in submarine groundwater discharge and associated nutrient transport into a tideless semi-enclosed embayment (Obama Bay, Japan). *Estuar Coasts* 39:13–26
- Sugimoto R, Kitagawa K, Nishi S, Honda H, Yamada M, Kobayashi S, Shoji J, Ohsawa S, Taniguchi M, Tominaga O (2017) Phytoplankton primary productivity around submarine groundwater discharge in nearshore coasts. *Mar Ecol Prog Ser* 563:25–33
- Turner SM, Malin G, Nightingale PD, Liss PS (1996) Seasonal variation of dimethyl sulphide in the North Sea and an assessment of fluxes to the atmosphere. *Mar Chem* 54:245–262
- Valiela I, Costa J, Foreman K, Teal JM, Howes B, Aubrey D (1990) Transport of groundwater-borne nutrients from watersheds and their effects on coastal waters. *Biogeochemistry* 10:177–197
- Wanninkhof R (1992) Relationship between wind speed and gas exchange over the ocean. *J Geophys Res Oceans* 97:7373–7382
- Waska H, Kim G (2010) Differences in microphytobenthos and macrofaunal abundances associated with groundwater discharge in the intertidal zone. *Mar Ecol Prog Ser* 407:159–172
- Waska H, Kim G (2011) Submarine groundwater discharge (SGD) as a main nutrient source for benthic and water-column primary production in a large intertidal environment of the Yellow Sea. *J Sea Res* 65:103–113
- Zhai W, Dai M, Cai WJ, Wang Y, Wang Z (2005) High partial pressure of CO₂ and its maintaining mechanism in a subtropical estuary: the Pearl River estuary, China. *Mar Chem* 93:21–32